Physics Letters A 596 (2026) 132148

Contents lists available at ScienceDirect

Physics Letters A

journal homepage: www.elsevier.com/locate/pla

Letter

Well-posed nonlocal anti-plane shear waves in a Zener piezoelectric viscoelastic half-space

Mohd Sadab [a,b], Yipin Su [a,b,*]

[a] Huanjiang Laboratory, Zhejiang University, Zhuji, 311800, China
[b] Department of Engineering Mechanics, Zhejiang University, Hangzhou, 310027, China

ARTICLE INFO

Communicated by Dr. MingZhong Wu

Keywords:
Anti-plane shear waves
Nonlocal elasticity
Well-posed boundary conditions
Zener model
Piezoelectric viscoelastic

ABSTRACT

The increasing demand for efficient vibration control and energy dissipation in aerospace structures has driven significant interest in smart viscoelastic materials with electromechanical coupling. As smart dampers, these materials detect unwanted vibrations and generate opposing forces to cancel them out, actively controlling structural dynamics. This study incorporates the nonlocal behavior of anti-plane shear waves with well-posed nonlocal boundary conditions, a topic that remains scarce in the literature. To address these issues, this article develops a novel governing equation for a piezoelectric viscoelastic material, based on the Zener model and nonlocal elasticity theory. The influence of shear moduli ratio on the phase velocity and attenuation with respect to the loss factor, is investigated numerically and graphically. A comparative analysis is further performed to assess the effect of the nonlocal parameter on phase velocity. The validity of the proposed model is confirmed by reducing the dispersion relation to a known limiting case.

1. Introduction

In recent decades, nonlocal elasticity theory has attracted significant attention due to its wide range of applications in nanotechnology, nanobeams, and thin-layered structures [1,2]. The application of nonlocal elasticity theory, originally proposed by Eringen and Edelen [3] and supported by earlier contributions [4,5], has experienced rapid growth in the mechanical modeling of such structures. To account for size-dependent effects in nanoscale systems, a nonlocal model based on Eringen's continuum theory has been developed.

In many of these studies, the research community has made a strong assumption that the integral and differential forms of nonlocal elasticity are equivalent. However, recent investigations have revealed inconsistencies in this assumption [6,7]. Specifically, it has been shown that solutions obtained from the differential form of nonlocal equations do not always satisfy the original integral formulations. For instance, recent work by Kaplunov et al. [8] demonstrated that the integral and differential models in nonlocal elasticity are not necessarily equivalent. In parallel, significant progress has been achieved through the development of stress-driven nonlocal elasticity. Romano and Barretta [9] proposed a stress-driven formulation that overcomes the well-posedness difficulties associated with the classical strain-driven Eringen model. While Pinnola et al. [10] established the equivalence between integral and differential stress-driven formulations and highlighted the role of constitutive boundary conditions in obtaining mathematically well-posed solutions. Unlike the stress-driven framework, the present study employs the asymptotically corrected differential nonlocal model proposed by Kaplunov and co-authors, which restores consistency between the integral and differential descriptions while retaining the convenience of a differential formulation. The current study is motivated by this critical observation and aims to fill this gap by introducing a Zener-based piezoelectric viscoelastic (ZPV) model within a well-posed nonlocal elasticity framework. This approach yields a novel governing equation. Another important aspect of this study involves the modeling of viscoelastic behavior. The Kelvin–Voigt model has been widely used in previous studies to describe the viscoelastic properties of piezoelectric materials [11,12]. But there are limits to this model, especially in terms of accurately capturing time-dependent effects. To address these shortcomings, more advanced viscoelastic formulations have been proposed in the literature. In particular, fractional-order viscoelastic models have attracted considerable attention owing to their ability to capture broadband dissipation and memory-dependent behavior more effectively than conventional integer-order models [13]. Despite their advantages, fractional-order formulations often lead to increased mathematical and computational complexity, especially when coupled with nonlocal elasticity theories. Therefore, in the present work, the classical Zener model is adopted to describe the viscoelastic behavior of the piezoelectric medium. The Zener model can simultaneously capture instantaneous elastic response

* Corresponding author.
E-mail address: su_yp@zju.edu.cn (Y. Su).

https://doi.org/10.1016/j.physleta.2026.132148
Received 3 June 2026; Received in revised form 28 July 2026; Accepted 1 September 2026
Available online 3 September 2026

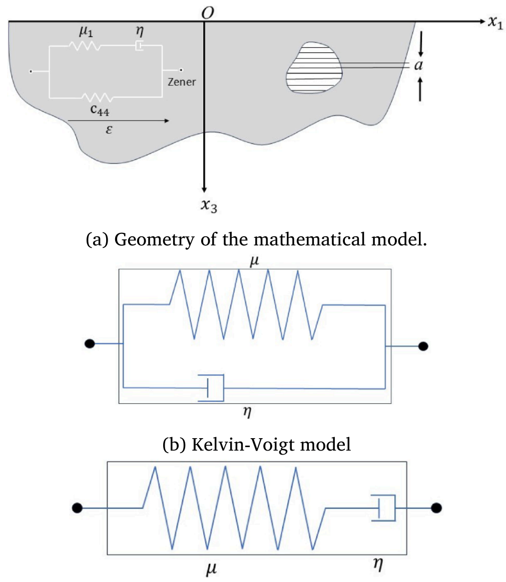

(a) Geometry of the mathematical model.

(b) Kelvin-Voigt model

(c) Maxwell model

Fig. 1. Schematic representations of viscoelastic models.

and long-term equilibrium behavior, making it better suited to realistic material modeling.

In this paper, we attempt to extend this well-posed nonlocal elasticity theory to a mathematical model of Zener model properties in piezoelectric-viscoelastic half-space. This Zener model allows for handling instantaneous events and long-term equilibrium simultaneously. The introduction of the shear moduli ratio and loss factor into nonlocal elastodynamics offers novel approaches and insights for theoretical exploration. A comparative study is also presented in this article, considering Kelvin–Voigt, Maxwell, and Zener models under nonlocality. Furthermore, curves illustrating the behavior of phase velocity and attenuation of anti-plane shear waves as a function of the operating loss factor of the ZPV half-space are obtained. The obtained dispersion relation is compared with the existing result to verify the authenticity and accuracy of the current model.

2. Theory and model

2.1. Geometric configuration of the mathematical model

Fig. (1a) illustrates the geometric configuration of the ZPV half-space considered in the present study, formulated within the framework of nonlocal elasticity theory. A Cartesian coordinate system Ox_1x_3 is introduced, where the x_1-axis denotes the direction of anti-plane shear wave propagation, and the x_3-axis is oriented vertically downward along the thickness direction. The origin O is located at the free surface of the half-space.

2.2. Basic equations

The balance laws of linear momentum together with the electric field equation based on nonlocal elasticity theory:

$$\sigma_{21,1} + \sigma_{23,3} = \rho(1 - a^2\nabla^2)\ddot{u}, \quad D_{1,1} + D_{3,3} = 0, \tag{1}$$

together with the traction-free and electrical boundary conditions at $x_3 = 0$:

$$\sigma_{23} - (a/2)\sigma_{12,1} + (a^2/2)\sigma_{12,13} + a^2\sigma_{12,33} = 0, \ \phi = 0, \tag{2}$$

where a (internal characteristic length), ρ (mass density), D (electric displacement), and ϕ (electric potential), while an overdot denotes differentiation with respect to time. The comma notation denotes partial differentiation with respect to the spatial coordinates. The corresponding local constitutive relations are given by:

$$\begin{aligned}(\mu_1 + \eta\partial_t)\sigma_{21} &= \mu_1 c_{44} u_{,1} + (\mu_1 + c_{44})\eta\partial_t(u_{,1}) + (\mu_1 + \eta\partial_t)e_{15}\phi_{,1},\\ (\mu_1 + \eta\partial_t)\sigma_{23} &= \mu_1 c_{44} u_{,3} + (\mu_1 + c_{44})\eta\partial_t(u_{,3}) + (\mu_1 + \eta\partial_t)e_{15}\phi_{,3},\end{aligned} \tag{3}$$

where η (viscosity), μ_1, c_{44} are the shear modulus, and ∂_t is the partial derivative with respect to time t. Furthermore, the electric displacement components take the form:

$$D_1 = e_{15}u_{,1} - \varepsilon_{11}\phi_{,1}, \quad D_3 = e_{15}u_{,3} - \varepsilon_{11}\phi_{,3}. \tag{4}$$

e_{15}, ε_{11} are the piezoelectric and dielectric coefficients. Substituting Eqs. (3) and (4) in Eq. (1), the governing equations:

$$\begin{aligned}&\left(c_{44}(\mu_1 + \eta\partial_t) + \mu_1\eta\partial_t\right)\nabla^2 u + (\mu_1 + \eta\partial_t)e_{15}\nabla^2\phi\\ &= \rho(\mu_1 + \eta\partial_t)(1 - a^2\nabla^2)u_{,tt}, \quad e_{15}\nabla^2 u - \varepsilon_{11}\nabla^2\phi = 0.\end{aligned} \tag{5}$$

Introducing the following transformations [14] defined as: $\psi = \phi - (e_{15}/\varepsilon_{11})u$, we obtain:

$$\begin{aligned}&\left(\bar{c}_{44}(\mu_1 + \eta\partial_t) + \mu_1\eta\partial_t\right)\nabla^2 u = \rho(\mu_1 + \eta\partial_t)(1 - a^2\nabla^2)u_{,tt}, \quad \nabla^2\psi = 0,\\ &\text{where, } \bar{c}_{44} = c_{44} + \frac{e_{15}^2}{\varepsilon_{11}}.\end{aligned} \tag{6}$$

2.3. Analytical solutions for the coupled equations

Assume the solutions of Eq. (6) as: $\{u, \psi\}(x_1, x_3, t) = \{u_p, \psi_p\}(x_3)\exp(i(kx_1 - \omega t))$, and substituting into Eq. (6), we obtain:

$$\left(\frac{d^2}{dx_3^2} - \beta_p^2\right)u_p(x_3) = 0, \quad \left(\frac{d^2}{dx_3^2} - k^2\right)\psi_p(x_3) = 0, \tag{7}$$

where: $\beta_p^2 = k^2 - k_p^2$, $k_p = \sqrt{\omega/c_p}$; ω denotes the angular frequency, while k represents the wavenumber. The complex anti-plane shear wave velocity in the ZPV half-space is given by $c_p = \sqrt{\mu_p/\rho}$. The complex shear modulus μ_p, embedded in c_p, follows the chosen viscoelastic constitutive equation:

$$\mu_p = \bar{c}_{44}\left(1 + \frac{\alpha\omega^2\delta^2}{\omega^2\delta^2 + \alpha^2} - i\frac{\omega\delta\alpha^2}{\alpha^2 + \omega^2\delta^2} - \frac{\rho\omega^2 a^2}{\bar{c}_{44}}\right). \tag{8}$$

The Zener time $\delta = \eta/\bar{c}_{44}$ marks the transition from elastic to viscous behavior, while $\alpha = \mu_1/\bar{c}_{44}$ denotes the shear moduli ratio. The real part of μ_p is the storage modulus, and the imaginary part is the loss modulus. Shear vibrations in the ZPV medium depend primarily on the loss factor $\omega\delta$ and the shear moduli ratio α.

Solving the above equations, the final displacement component and electric potential function can be found as:

$$\begin{aligned}u(x_1, x_3, t) &= A_p\exp(-\beta_p x_3)\exp(i(kx_1 - \omega t)), \quad \phi(x_1, x_3, t)\\ &= \left(B_p\exp(-kx_3) + \frac{e_{15}}{\varepsilon_{11}}A_p\exp(-\beta_p x_3)\right)\exp(i(kx_1 - \omega t)).\end{aligned} \tag{9}$$

where A_p and B_p are the arbitrary constants.

2.4. Dispersion relation and validation

By incorporating the relevant mechanical, electrical displacement, and stress components into the boundary conditions, we derive the subsequent homogeneous algebraic system of equations as:

$$D_1 + D_2 - \frac{iak}{2}(C_1 + C_2) + a^2k^2C_1\left(1 - \frac{i}{2}\right) + a^2\beta_p C_2\left(\beta_p - \frac{ik}{2}\right) = 0, \tag{10}$$

$$e_{15}A_p + \varepsilon_{11}B_p = 0, \tag{11}$$

where: $C_1 = ik\mu_1 e_{15}B_p + k\omega\eta e_{15}B_p$, $C_2 = ik\mu_1 c_{44}A_p + ik\mu_1\frac{e_{15}^2}{\varepsilon_{11}}A_p + k\omega\eta(\mu_1 + c_{44})A_p + k\omega\eta\frac{e_{15}^2}{\varepsilon_{11}}A_p$,

$D_1 = -ke_{15}(\mu_1 - i\omega\eta)B_p$, $D_2 = -\beta_p\mu_1 c_{44}A_p + i\omega\beta_p\eta(\mu_1 + c_{44})A_p - \beta_p\frac{e_{15}^2}{\varepsilon_{11}}(\mu_1 - i\omega\eta)A_p$.

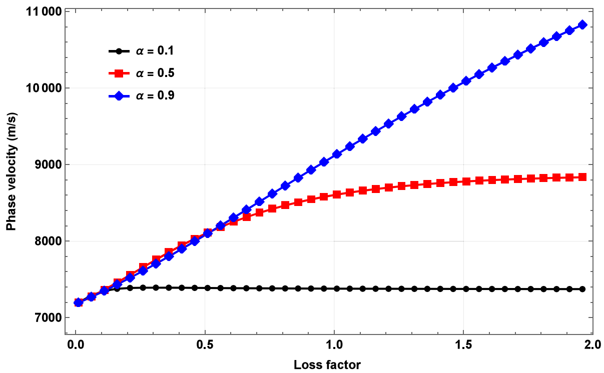

(a)

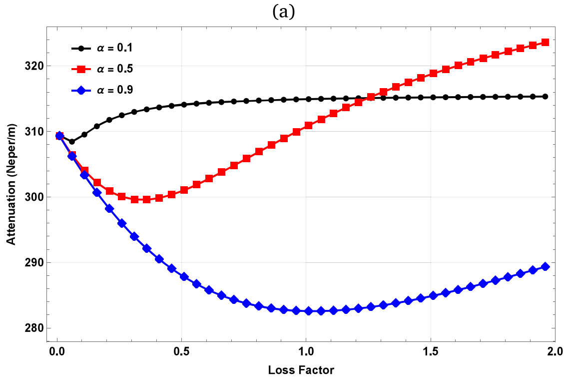

(b)

Fig. 2. Influence of shear moduli ratio on phase velocity and attenuation of anti-plane shear waves with respect to loss factor.

If the half-space is free from piezoelectricity, then the dispersion reduces to anti-plane shear wave propagation in a nonlocal Zener viscoelastic medium:

$$D_2 - \frac{iak}{2}C_2 + a^2\beta_p C_2\left(\beta_p - \frac{ik}{2}\right) = 0. \tag{12}$$

This limiting case confirms that the viscoelastic contribution appears consistently in the present formulation. Furthermore, if the above dispersion relation is free from viscoelasticity, Eq. (12) reduces to the nonlocal elastic formulation. The resulting dispersion relation coincides with Eq. (82) of Kaplunov et al. [8].

$$C = \sqrt{1 - \frac{K^2}{4}}, \text{ where, } C = c/c_p \text{ and } K = ak. \tag{13}$$

2.5. Kelvin–Voigt model

In Fig. (1b), the Kelvin–Voigt framework, the viscoelastic medium is modeled as a parallel combination of an elastic spring and a viscous dashpot. The resulting complex shear modulus is given by:

$$\mu = \mu_0 - i\omega\eta = \mu_0(1 - i\tan\delta), \tag{14}$$

where: $\tan\delta = \frac{\omega\eta}{\mu_0}$ represents the loss factor, which quantifies the energy dissipation and is equivalent to the inverse quality factor Q^{-1}.

2.6. Maxwell model

In the Maxwell model shown in Fig. (1c), the spring and dashpot are connected in series. The corresponding complex shear modulus takes the form:

$$\mu = \mu_0\left(\frac{(\omega\theta)^2}{1+(\omega\theta)^2} - i\frac{\omega\theta}{1+(\omega\theta)^2}\right), \tag{15}$$

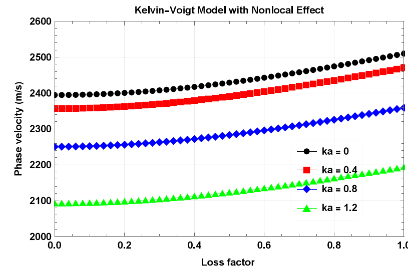

(a)

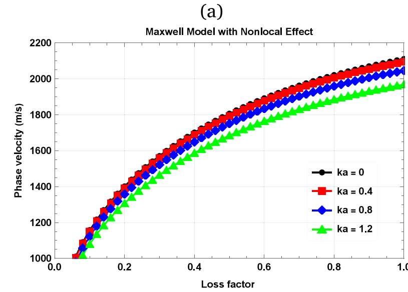

(b)

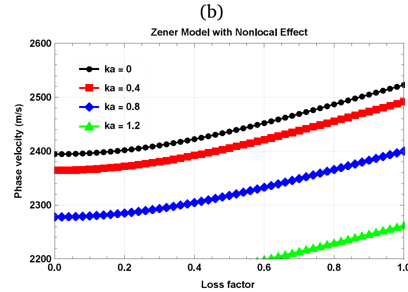

(c)

Fig. 3. Influence of nonlocal parameter for (a) Kelvin-Voigt, (b) Maxwell, and (c) Zener models on phase velocity with respect to loss factor.

where: $\theta = \frac{\eta}{\mu_0}$ denotes the relaxation time. The real and imaginary parts of μ represent the elastic and dissipative responses, respectively, and play a central role in governing wave dispersion and attenuation.

3. Results and discussion

The phase velocity and attenuation characteristics of shear waves are analytically evaluated. Their behavior is illustrated through graphical and numerical simulations based on the material parameters of $BaTiO_3$ [15]: $c_{44} = 43 \times 10^9$ N/m^2, $\varepsilon_{11} = 11.2 \times 10^{-9}$ C^2/N $\cdot$ m^2, $\rho = 5.3 \times 10^3$ kg/m^3, and $e_{15} = 12.7$ C/m^2. Fig. (2) shows the effect of the shear modulus ratio parameter α on the phase velocity and attenuation characteristics of anti-plane shear waves against the loss factor. It is noticed that for the first value of shear moduli ratio, i.e., $\alpha = 0.1$, the phase velocity exhibits almost the same behavior with very minor variations, indicating a lower sensitivity of the wave propagation speed to the loss factor at lower shear modulus ratios. In contrast, for $\alpha = 0.5$, the phase velocity increases monotonically with the loss factor and reaches a saturation level at higher values of the loss factor. A more pronounced increase is observed for $\alpha = 0.9$, where the phase velocity increases almost linearly, indicating that a higher shear modulus ratio significantly increases the wave propagation speed and amplifies the effect of dissipation-related parameters. It is found that for $\alpha = 0.1$ the attenuation decreases slightly at first and then remains almost constant, indicating a weak dependence on dissipation. The attenuation curves show a non-monotonous behavior. This suggests a transition from dominant elastic effects to dissipation-controlled wave behavior. For $\alpha = 0.9$, attenuation first decreases rapidly and then increases slowly, but remains lower than in other cases in the intermediate range of loss factor. Over-all, the results clearly show that the shear modulus ratio plays a significant role in controlling both the phase velocity and attenuation of anti-plane shear waves. Higher values of α intensify the interaction between material stiffness and dissipative effects, increasing the sensitivity of wave characteristics to loss factor. These observations are essential for the design of advanced smart and graded materials, where control over wave propagation and attenuation is required. Fig. (3) shows the effect of the nonlocal parameter ka on the phase velocity of anti-plane shear waves for (a) Kelvin–Voigt, (b) Maxwell, and (c) Zener models as a function of the loss factor. For the results presented in the Fig. (3), the piezoelectric coupling effects are neglected, whereas the nonlocal parameter is retained to examine the influence of different viscoelastic models on wave propagation characteristics. The phase velocity progressively rises with the loss factor for all values of ka. However, increasing ka consistently reduces the phase velocity, indicating the softening effect induced by nonlocality. The variation remains smooth due to the dominant viscous damping behavior of the Kelvin–Voigt model. The Maxwell model exhibits a rapid increase in phase velocity at higher loss factors, while a tendency toward saturation is observed at lower loss factors. Finally, the nonlocal parameter significantly affects wave propagation, reducing the phase velocity in all models, while the largest effect is observed in the case of the Zener model.

4. Conclusion

The results obtained for layered viscoelastic waveguides characterized by the Zener model have significant applications in various fields of science and technology, including geophysics and non-destructive testing. Furthermore, they are useful for interpreting experimental observations of Love wave propagation characteristics in viscoelastic waveguides.

CRediT authorship contribution statement

Mohd Sadab: Writing – review & editing, Writing – original draft, Visualization, Validation, Software, Methodology, Investigation, Conceptualization; **Yipin Su:** Writing – review & editing, Supervision, Resources, Formal analysis.

Declaration of competing interest

The authors declare that they have no known competing financial interests or personal relationships that could have appeared to influence the work reported in this paper.

Acknowledgment

This work was funded by the National Natural Science Foundation of China (grant no 12402193) and the National Natural Science Foundation of Zhejiang Province (grant no LR26A020003).

Data availability

No data was used for the research described in the article.

References

[1] T. Aksencer, M. Aydogdu, Levy type solution method for vibration and buckling of nanoplates using nonlocal elasticity theory, Phys. E: Low-Dimens. Syst. Nanostruct. 43 (4) (2011) 954–959.
[2] H.-T. Thai, T.P. Vo, T.-K. Nguyen, S.-E. Kim, A review of continuum mechanics models for size-dependent analysis of beams and plates, Compos. Struct. 177 (2017) 196–219.
[3] A.C. Eringen, D. Edelen, On nonlocal elasticity, Int. J. Eng. Sci. 10 (3) (1972) 233–248.
[4] L.L. Zhang, J.X. Liu, X.Q. Fang, G.Q. Nie, Effects of surface piezoelectricity and nonlocal scale on wave propagation in piezoelectric nanoplates, Eur. J. Mech.-A/Solid. 46 (2014) 22–29.
[5] S. Manna, M. Bhat, Love wave fields in a non-local elastic model with reinforced and inhomogeneous media, Soil Dyn. Earthq. Eng. 161 (2022) 107388.
[6] O. Şahin, An asymptotic formulation for boundary value problems in a non-local elastic half-space, Acta Mech. 235 (4) (2024) 2061–2075.
[7] J. Kaplunov, D.A. Prikazchikov, L. Prikazchikova, On non-locally elastic Rayleigh wave, Philos. Trans. R. Soc. A: Math. Phys. Eng. Sci. 380 (2231) (2022).
[8] J. Kaplunov, D.A. Prikazchikov, L. Prikazchikova, On integral and differential formulations in nonlocal elasticity, Eur. J. Mech.-A/Solid. 100 (2023) 104497.
[9] G. Romano, R. Barretta, Nonlocal elasticity in nanobeams: the stress-driven integral model, Int. J. Eng. Sci. 115 (2017) 14–27.
[10] F.P. Pinnola, S.A. Faghidian, R. Barretta, F.M. de Sciarra, Variationally consistent dynamics of nonlocal gradient elastic beams, Int. J. Eng. Sci. 149 (2020) 103220.
[11] J. Chen, J. Yu, L. Elmaimouni, B. Zhang, H. Tu, Rayleigh waves in viscoelastic piezoelectric half-space with cladding structures: an analytic Legendre-Laguerre polynomial method, Eur. J. Mech.-A/Solid. 107 (2024) 105397.
[12] C. Xu, C. Niu, A. Jan, Y. Yu, A symplectic elasticity approach for precise fracture analysis of V-notched visco-piezoelectric/elastic bimaterials, Eur. J. Mech.-A/Solid. (2025) 105912.
[13] R. Barretta, F. Marotti de Sciarra, F.P. Pinnola, M.S. Vaccaro, On the nonlocal bending problem with fractional hereditariness, Meccanica 57 (4) (2022) 807–820.
[14] J.L. Bluestein, A new surface wave in piezoelectric medium, Appl. Phys. Lett. 13 (1968) 412–413.
[15] Y. Pang, J.-X. Liu, Y.-S. Wang, X.-F. Zhao, Propagation of Rayleigh-type surface waves in a transversely isotropic piezoelectric layer on a piezomagnetic half-space, J. Appl. Phys. 103 (7) (2008).